



ELSEVIER

Journal of Electron Spectroscopy and Related Phenomena 108 (2000) 203–211

JOURNAL OF
ELECTRON SPECTROSCOPY
and Related Phenomena

www.elsevier.nl/locate/elspec

Time-resolved dynamics of charge transfer to solvent states in solvated iodide clusters

Alison V. Davis, Martin T. Zanni, Christian Frischkorn, Daniel M. Neumark*

Department of Chemistry, University of California, and Chemical Sciences Division, Lawrence Berkeley National Laboratory, Berkeley, CA 94720, USA

Abstract

The dynamics of the cluster precursors to charge-transfer-to-solvent (CTTS) states have been studied in clusters of iodide with xenon, water, D_2O , ammonia and methanol using femtosecond photoelectron spectroscopy. The dynamics of these states differ dramatically according to solvent type and number. Excitation of the lower CTTS state in $I^-(Xe)_n$ clusters yields a state that is stable over the time scale of the experiment (~ 200 ps), whereas the upper spin-orbit state decays by spin-orbit autodetachment within 500 to 1000 fs, depending on the number of Xe atoms. The hydrogen-bonded clusters show evidence for partial solvation of the excess electron following CTTS excitation. In general they exhibit more complicated dynamics which correspond to internal rearrangement in one or more electronic states. A description including isomerization and electron solvation is given for the $I^-(D_2O)_n$ clusters, and compared to the dynamics observed in $I^-(NH_3)_n$ and $I^-(CH_3OH)_n$ clusters. © 2000 Elsevier Science B.V. All rights reserved.

Keywords: Clusters; Photoelectron spectroscopy; Time-resolved dynamics; Solvated electrons

1. Introduction

An electron is one of the simplest solutes, yet displays a rich variety of dynamics in liquid solvents as varied as xenon and water. One of the more elegant ways to generate solvated electrons is by photodetachment of anions in solution. In 1928, Franck et al. observed two ultraviolet absorption bands in dilute aqueous iodide solution [1] spaced by the spin-orbit splitting in atomic iodine. These charge-transfer-to-solvent (CTTS) bands [2] were attributed to excitation of an electron from a localized orbital on the iodide anions to a relatively delocalized orbital in which the electron is interact-

ing with both the resulting iodine atom and the surrounding solvent species, ultimately resulting in the production of solvated electrons [3,4]. The dynamics by which the electron leaves the anion through the CTTS state and becomes stabilized in the solvent have been investigated in water by various experimental groups [5–7] using femtosecond absorption studies, and by theory groups using molecular dynamics simulations [8,9].

Since CTTS bands do not exist in isolated (i.e. gas phase) iodide anions, it is of interest to understand how these bands are manifested in finite clusters. In other words, how large a cluster is required before these bands appear, and what are the associated dynamics? Johnson et al. [10] observed diffuse electronic bands in $I^-(H_2O)_{n=1-4}$ clusters just above the detachment threshold to the lower ($^2P_{3/2}$) state of the neutral $I\cdot(H_2O)_n$ cluster. These states shifted to

*Corresponding author. Tel.: +1-510-642-3502; fax: +1-510-642-6262.

E-mail address: dan@radon.cchem.berkeley.edu (D.M. Neumark)

higher energy with increasing n , appearing to converge to the lower CTTS band of iodide in aqueous solution, and were therefore assigned to cluster precursors to the lower CTTS band. Cheshnovsky and co-workers [11,12] have observed similar bands in $I^-(Xe)_{n=4-54}$; clusters with four or more Xe atoms show two well-separated bands which are assigned to the lower ($I(^2P_{3/2})Xe_n^-$) and upper ($I(^2P_{1/2})Xe_n^-$) spin-orbit states of the electronically excited cluster. The picture implied by these studies is shown in Fig. 1, where we expect an excited state of the anion near each of the detachment thresholds to the two spin-orbit levels of the neutral cluster.

We have gained a complementary perspective to these spectroscopic works by using femtosecond photoelectron spectroscopy (FPES) to study the dynamics of small gas-phase clusters excited to CTTS states. In our technique, a gas-phase $I^-(S)_n$ cluster, where S is a solvent atom or molecule, is excited to a CTTS state by a femtosecond laser pulse (the pump pulse) of appropriate wavelength. This is shown in Fig. 1 for excitation to the lower CTTS band. The excited cluster is then probed after a time delay by a second femtosecond pulse (the probe pulse) that detaches the electron, and the resulting photoelectron spectrum is measured. By examining

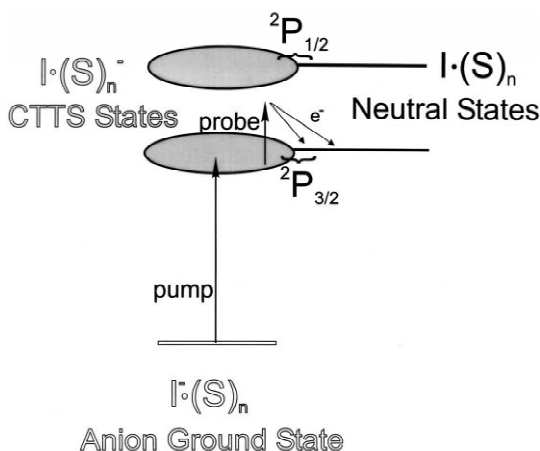


Fig. 1. Schematic diagram of the energy levels involved in the experiments reported herein. S represents one of the five types of solvent molecules listed in the text. The anion ground and CTTS states are represented by outlined levels; the neutral levels are solid lines. The pump energy shown here corresponds to excitation of the lower CTTS band; in Xe clusters, the upper level was excited as well.

the CTTS dynamics of several types of solvent molecules in this way, we can probe how the number and type of solvent species influence the dynamics of electron solvation. Previously we have reported results for $I^-(H_2O)_n$ clusters. These are summarized here and compared to FPE spectra for clusters of iodide solvated by other species: $I^-(Xe)_n$, $I^-(NH_3)_n$, and $I^-(CH_3OH)_n$.

2. Experimental

Our experimental apparatus has been described in detail elsewhere [13]; only a brief summary is given here. $I^-(\text{solvent})_n$ clusters are formed in a supersonic expansion of an appropriate carrier gas mixed with and/or passed over a source for the solvent molecules, and subsequently passed over a reservoir of CH_3I . The resulting mixture is expanded through a pulsed molecular beam valve and crossed by a 1.6 keV electron beam just downstream of the valve orifice. For the $I^-(Xe)_n$ clusters, the mixture is 4% Xe in 2 bar Ar; for the $I^-(NH_3)_n$ clusters, 0.9% NH_3 in 1.5 bar Ar. One bar Ar is passed over D_2O prior to the CH_3I reservoir to make $I^-(D_2O)_n$ clusters, and $I^-(CH_3OH)_n$ clusters are produced by 1.5 bar N_2 flowed over CH_3OH before the CH_3I . Anions produced by the electron gun are injected into and size-selected by a Wiley–McLaren time-of-flight mass spectrometer. After passing through several differentially pumped regions, clusters of the desired mass are excited and photodetached by the femtosecond pump and probe laser pulses at the focus of a magnetic bottle photoelectron spectrometer. A reflectron mass analyzer downstream from the laser interaction region can be used to identify ionic photofragments.

The pump and probe pulses are produced from a Clark-MXR regeneratively amplified Ti:Sapphire laser system that generates tunable 80 fs (FWHM; sech^2), 1 mJ pulses in the range 790–825 nm at a repetition rate of 500 Hz. About 200 μJ of this fundamental output is used as the probe pulse; the rest is used to generate the UV pump pulse. The near-IR probe pulse passes through a translation stage to vary the pump-probe delay. The pump photon energy must be resonant with the CTTS band in the cluster and was tuned in two ways, enabling us

to access the lower and upper spin-orbit states of $I^-(Xe)_n$ clusters and the lower spin-orbit state for the other clusters. The frequency of the fundamental can be tuned prior to frequency tripling, yielding 12 μJ of 275 to 263 nm (4.51 to 4.71 eV) pulses with a FWHM of 120 fs. This was used as the excitation wavelength for the $I^-(D_2O)_n$, $I^-(CH_3OH)_n$, large $I^-(NH_3)_n$, and excitation of $I^-(Xe)_n$ clusters to the upper spin-orbit state. Longer-wavelength excitation pulses were created by using 790 nm pulses to pump a TOPAS tunable optical parametric amplifier (Quantronix), whose output is frequency-quadrupled, yielding 4 μJ pulses with wavelength ranging from 369 to 344 nm (110 fs FWHM). These were used to pump the smaller $I^-(NH_3)_n$ clusters and the lower spin-orbit band of $I^-(Xe)_n$ clusters.

3. Results

3.1. $I^-(Xe)_n$ clusters

$I^-(Xe)_n$ clusters were excited by laser pulses within 20 meV of the energies determined by Becker et al. [11] for the CTTS bands. Both upper and lower spin-orbit states were studied.

Fig. 2a shows photoelectron spectra of $I^-(Xe)_{11}$ excited to the ${}^2P_{1/2}$ (upper spin orbit) CTTS band by 4.55 eV light. The data are presented as a contour plot, with pump-probe delay on the x axis, electron kinetic energy on the y axis, and intensity indicated by color density. The shape of the photoelectron spectrum does not vary with time; only its overall intensity changes. After peaking around 200 fs, the photoelectron intensity gradually decays. Fig. 2b plots the integrated photoelectron intensity as a function of time for the $n=11$, 20, and 38 clusters. The data were fitted to exponential decay functions with time constants as shown. The excited state lifetime clearly increases with cluster size, with about a factor of two difference between the $n=11$ and $n=38$ clusters.

$I^-(Xe)_{n=6-13}$ clusters were also excited to the ${}^2P_{3/2}$ (lower spin-orbit) CTTS band. Here too the photoelectron spectrum shape does not change with time, but there is also no decay measurable within 225 ps. This can be seen in Fig. 2c, which shows the integrated photoelectron intensity as a function of

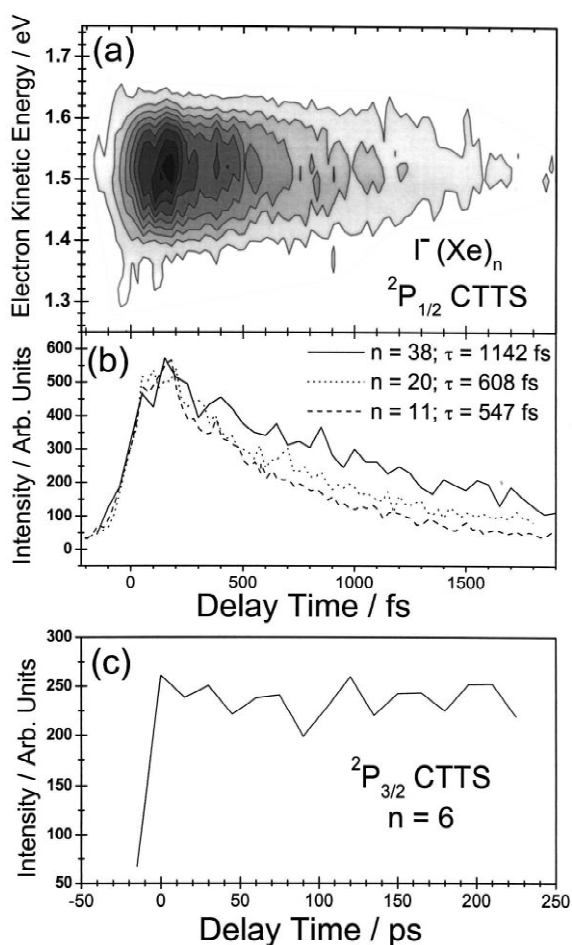


Fig. 2. (a) Femtosecond photoelectron (FPE) spectra as a function of pump-probe delay of $I^-(Xe)_{11}$ excited to the upper CTTS state by 272-nm light. Darkness corresponds to photoelectron intensity. (b) Integrated intensity of photoelectron peak for $I^-(Xe)_n$ ($n=11, 20, 38$) clusters in the ${}^2P_{1/2}$ CTTS states. Time constants for exponential decay of intensity are given. (c) Integrated intensity of the photoelectron peak for $I^-(Xe)_6$ excited to the ${}^2P_{3/2}$ CTTS state.

time for $I^-(Xe)_6$ excited to the lower CTTS state using 363-nm light. Larger clusters (not shown) also did not decay.

3.2. $I^-(D_2O)_n$

The dynamics of CTTS excitation in $I^-(D_2O)_n$ have been discussed in detail in Lehr et al. [14]; only a brief summary is given here. The photoelectron

spectra of $I^-(D_2O)_n$ ($n=4-6$) clusters excited to the $^2P_{3/2}$ CTTS band by 263-nm light are shown in Fig. 3. These spectra are much more complicated than those of the xenon clusters. The photoelectron spectrum of $I^-(D_2O)_4$ resembles Fig. 2a, the spectrum of $I^-(Xe)_{11}$ excited to the upper spin-orbit state. Like the $I^-(Xe)_n$ clusters, its spectrum shape does not change much with time, although there is an initial rapid shift of 0.07 eV to lower energies; this shift continues slightly over longer times. The integrated intensity peaks around 200 fs and then decays with a time constant of 2.8 ps.

In contrast, the spectrum of $I^-(D_2O)_5$ is centered around 1.45 eV for the first 3–400 fs and then shifts abruptly by 0.21 eV toward lower electron energy, with a time constant for the shift of 390 fs. Its intensity grows in this second region at lower electron kinetic energy, peaking around 2.3 ps.

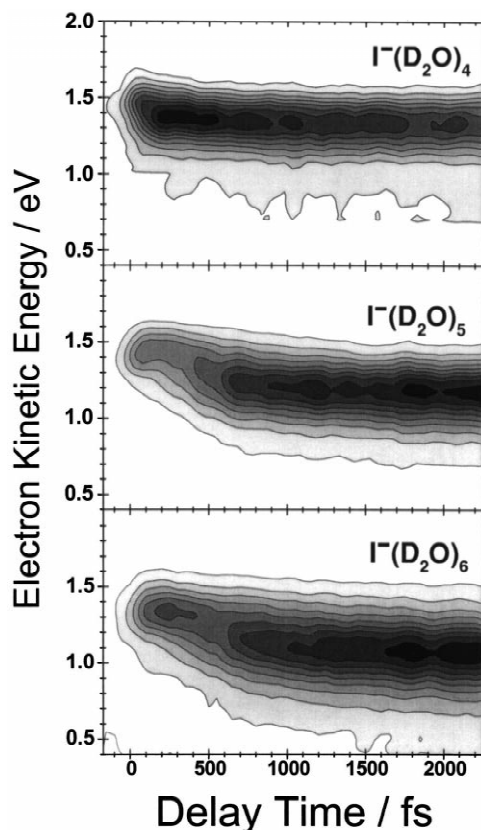


Fig. 3. FPE spectra as a function of pump-probe delay of $I^-(D_2O)_n$ ($n=4-6$).

$I^-(D_2O)_6$ behaves similarly, with a larger shift and associated time constant (0.28 eV and 560 fs, respectively). The integrated photoelectron intensity for both clusters ultimately decays with exponential time constants given in Table 1; these are considerably longer than for $I^-(D_2O)_4$.

3.3. $I^-(NH_3)_n$

The photoelectron spectra of $I^-(NH_3)_n$ ($n=4-6, 8$) are shown in Fig. 4. For $n=4, 5, 6, 8$, the excitation wavelengths were 321 nm, 319 nm, 313 nm, and 270 nm, respectively. As for the water clusters, the important features are the eKE peak position and intensity. All clusters show some degree of shifting to lower eKE, and as the cluster size gets larger, this shift increases. For $I^-(NH_3)_n$ ($n=4, 5, 6$) the shift is 0.069, 0.097, 0.117 eV, respectively. The shift continues to increase, and in $I^-(NH_3)_8$ it is 0.211 eV. This shift begins immediately after excitation in contrast to the delay seen in the $I^-(D_2O)_n$ ($n \geq 5$) cluster spectra. For each cluster size, the integrated intensity of the eKE peak increases with delay time, reaching a maximum between 1 and 2 ps, and at later times (not shown) exhibiting slow exponential decay with the time constants listed in Table 1.

3.4. $I^-(CH_3OH)_n$

FPE spectra for $I^-(CH_3OH)_n$ ($n=5-7$) clusters at delay times less than 2 ps are shown in Fig. 5. These were obtained with a pump wavelength of 263 nm which excites the lower CTTS band. These spectra are similar to those of $I^-(NH_3)_n$, with a shift toward lower energy beginning immediately, and the size of the shift increasing with n . The magnitudes of the

Table 1
Long-time decay of CTTS states^a

	$I^-(H_2O)_n$	$I^-(NH_3)_n$	$I^-(CH_3OH)_n$
$n=4$	2.8 ps	12	
5	37	21	4.5
6	96	22	10
7	300		19
8		28	22

^a Exponential decay time constants (ps) for several I^- hydrogen-bonded clusters.

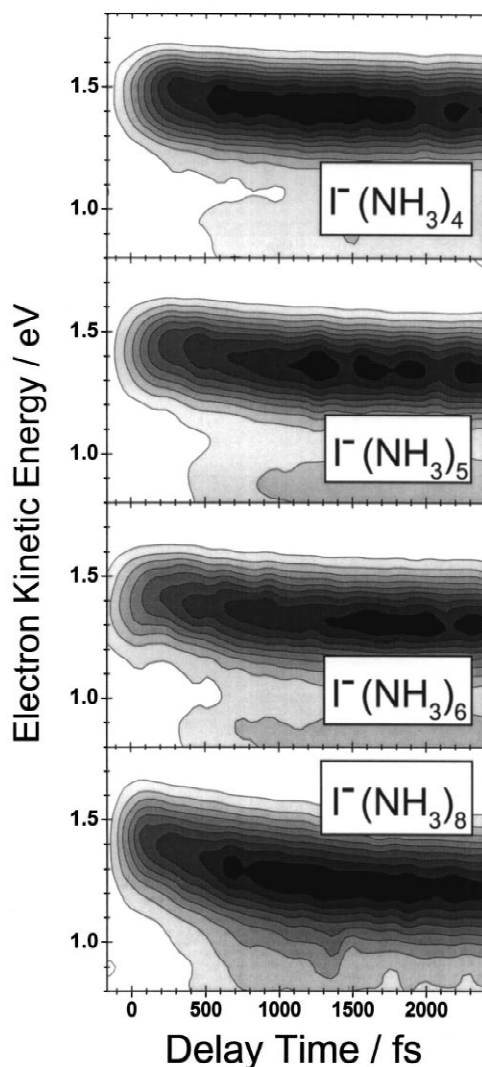


Fig. 4. FPE spectra of $\text{I}^-(\text{NH}_3)_n$ ($n=4-6, 8$).

shift for $\text{I}^-(\text{CH}_3\text{OH})_n$ ($n=5, 6, 7$) are 0.075, 0.091, and 0.126 eV, respectively. The photoelectron intensity of $\text{I}^-(\text{CH}_3\text{OH})_5$ peaks early and decays, while that for $\text{I}^-(\text{CH}_3\text{OH})_n$ ($n \geq 6$) peaks later, around 1.5 ps.

At long times the dynamics differ significantly from those observed in water or ammonia clusters. The FPE spectra of $\text{I}^-(\text{CH}_3\text{OH})_n$ ($n=5-7$) are presented in Fig. 6 for delay times up to 50 ps, with spectra taken every picosecond. After about 2 ps, the photoelectron peak stops shifting to lower energies,

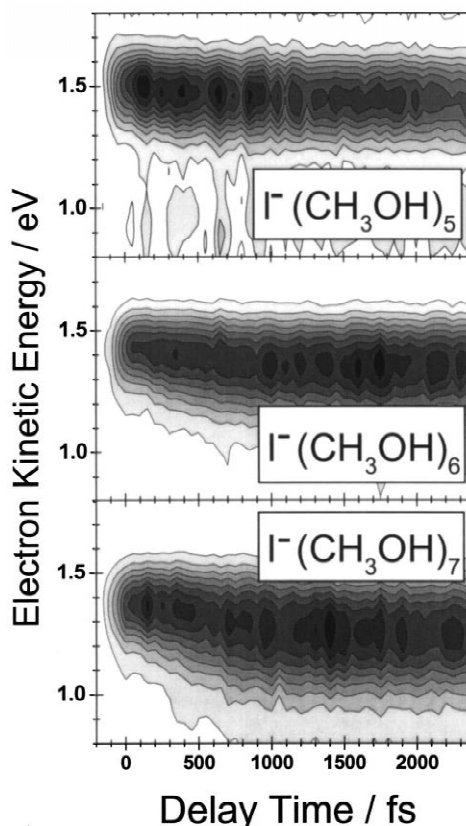


Fig. 5. FPE spectra of $\text{I}^-(\text{CH}_3\text{OH})_n$ ($n=5-7$) at times less than 2500 fs.

and begins shifting back to higher eKE, even (for $n=7$) surpassing the average energy at 0 ps. In Fig. 7 the peak position for these clusters is plotted against delay time. As the spectra shift back to higher energy, they also decay with characteristic time constants given in Table 1.

4. Discussion

The FPE spectra of the clusters presented here show substantial variation with the solvent composition. For the $\text{I}^-(\text{Xe})_n$ clusters, excitation to the lower spin-orbit CTTS state shows no dynamics at all, whereas excitation to the upper state results in spectra that decay on a time-scale of 500–1000 fs, with no change in the electron kinetic energy during this time. For a given cluster, the only difference

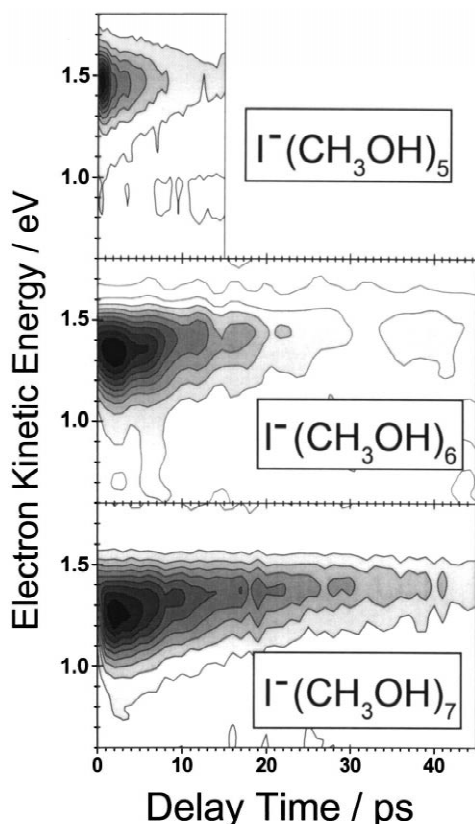
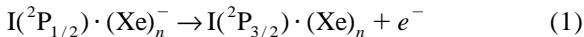


Fig. 6. FPE spectra of $I^-(CH_3OH)_n$ ($n=5-7$) at times less than 45 ps.

between the two CTTS states is the spin-orbit level of the I atom in the cluster. We therefore attribute the decay of the upper state to spin-orbit-induced autodetachment, i.e.



This route of decay is, of course, unavailable to the lower spin-orbit CTTS state which, in any event, is probably slightly bound with respect to the detachment continuum [11,15]. Eq. (1) requires that the excess electron interacts with the I atom in order to induce a spin-flip; the increase in lifetime with n (Fig. 2b) indicates that this interaction is less likely for clusters with more Xe atoms. The absence of any shifting of the electron kinetic energy indicates that

relatively little solvent rearrangement occurs to stabilize the excess electron, in contrast to all the other clusters studied here.

The dynamics of $I^-(D_2O)_n$ clusters subsequent to excitation to the lower CTTS band are much more complicated than those of $I^-(Xe)_n$ clusters, and are discussed in detail in Lehr et al. [14]. Briefly, we attribute the initial CTTS excitation to a dipole bound state supported by the solvent network [10]. For $I^-(D_2O)_4$, slight rearrangement and vibrational relaxation occurs in this state, and it decays by vibrational autodetachment. For $n \geq 5$, after a few hundred femtoseconds in the dipole-bound state, the cluster undergoes a transition to a new electronic state which has a larger electron affinity, causing the photoelectron spectrum to shift to lower energies. A qualitative potential surface for this process is shown in Fig. 8a. After this shift, the photoelectron intensity increases, indicating that the new electronic state has a higher cross section for detachment, typical of an anion state with the excess electron localized and more strongly bound [16]. For this reason, we believe this new electronic state has ‘partially solvated’ character, with the electron more localized within the solvent network. But the intensity increase does not coincide with the timing of the photoelectron spectrum shift, suggesting that vibrational redistribution in the cluster is necessary to fully localize the excess electron. A similar trend is found in both $I^-(NH_3)_n$ and $I^-(CH_3OH)_n$ clusters, discussed below.

The dynamics of the CTTS band of $I^-(NH_3)_n$, though similar in some ways to those of the water clusters, exhibit some significant differences. Dipole-bound states are less likely to be important; no dipole-bound $(NH_3)_n^-$ anions have been found experimentally or theoretically. The $I^-(NH_3)_n$ spectra begin shifting to lower energies immediately after excitation, suggesting that, in fact, there is no metastable dipole bound state as found in the $I^-(D_2O)_n$ clusters, and that only one electronic state is being accessed, as pictured qualitatively in Fig. 8b. The gradual onset of shifting of the photoelectron spectra in $I^-(NH_3)_n$ clusters indicates that there is no critical n for solvation in the range studied, in contrast to $I^-(D_2O)_n$ where partial solvation does not occur until five solvent molecules are present.

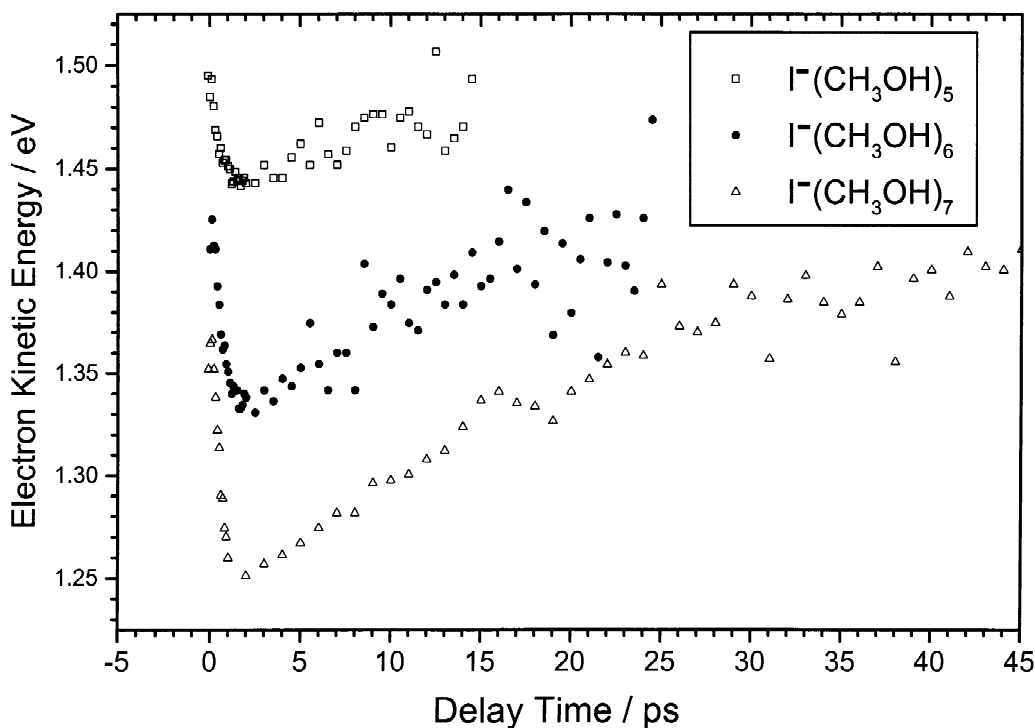


Fig. 7. Average electron kinetic energy of $\text{I}^-(\text{CH}_3\text{OH})_n$ ($n=5-7$) out to 45 ps. The initial shifts to lower eKE, and the shifting back to higher eKE, are illustrated.

The differences between $\text{I}^-(\text{NH}_3)_n$ and $\text{I}^-(\text{D}_2\text{O})_n$ are further emphasized in Table 1, which shows that the long-time decay of the electron signal from $\text{I}^-(\text{NH}_3)_n$ increases slowly with n , whereas that for $\text{I}^-(\text{D}_2\text{O})_n$ increases by more than a factor of 10 from $n=4$ to $n=5$.

The FPE for $\text{I}^-(\text{CH}_3\text{OH})_n$ clusters at short times are more similar to those for $\text{I}^-(\text{NH}_3)_n$ than to $\text{I}^-(\text{D}_2\text{O})_n$ clusters. The solvation shift increases gradually with cluster size, and there is no clear evidence for an initially excited dipole-bound state. The most unique feature of $\text{I}^-(\text{CH}_3\text{OH})_n$ clusters is their long-term behavior shown in Figs. 6 and 7. The shifting of the average eKE toward higher energy between 2 and 50 ps is not seen to any significant extent in the $\text{I}^-(\text{D}_2\text{O})_n$ or $\text{I}^-(\text{NH}_3)_n$ clusters. The way in which this shift occurs is interesting. The FPE spectra are clearly broader at 2–5 ps than at longer times, and the narrowing that occurs at longer

times is quite asymmetric; the upper edge of each contour remains at approximately constant eKE, while the lower edge shifts to higher eKE. It is possible that this shifting and narrowing is due to evaporative loss of a solvent molecule or the I atom. Alternatively, there may be two solvent configurations contributing to the signal around 2 ps, one of which has a significantly shorter lifetime than the other. The interpretation of the FPE spectra would be greatly aided by infrared spectroscopy experiments and electronic structure calculations so that, at the very least, the initial structures of the $\text{I}^-(\text{CH}_3\text{OH})_n$ would be better known.

Finally, we address the long-term exponential decay of photoelectron intensity that is seen in all the clusters. In solution, decay of solvated electron signal is attributed to recombination with the iodine atom [7–9]. If this were to happen in our experiment, the energy released would result in fragmentation of

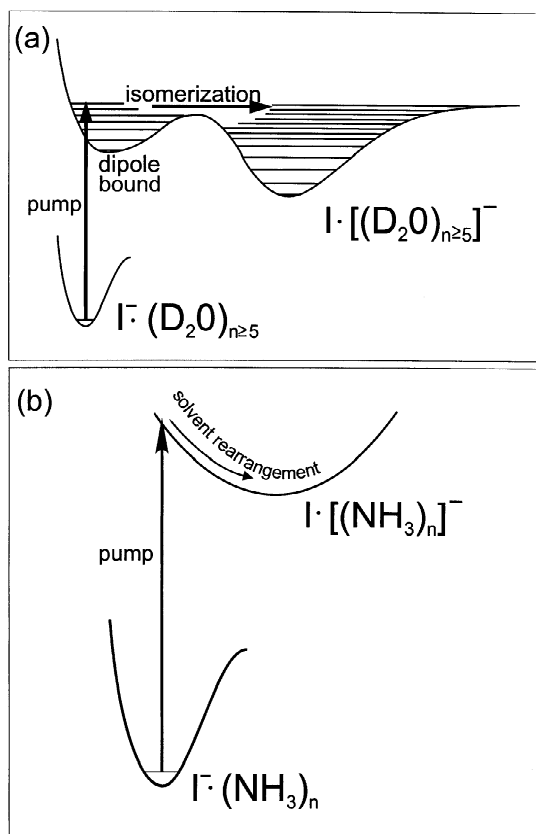


Fig. 8. Schematic picture of dynamics on the $I^-(D_2O)_n$ and $I^-(NH_3)_n$ clusters' potential surfaces. (a) $I^-(D_2O)_n$ clusters: at $t=0$, the pump excites the cluster to the dipole bound state. For $n=4$, only this well exists; the cluster remains in it, decaying by vibrational autodetachment. For $n \geq 5$, the cluster remains in this well for a few hundred femtoseconds before isomerizing to a nearby 'solvated electron' state with a geometry similar to $I \cdot [(D_2O)_n]^-$. (b) $I^-(NH_3)_n$ clusters: at $t=0$, the pump excites the cluster directly to the partially solvated state, where it vibrationally relaxes.

the cluster, leading to daughter ions which could be detected with our reflectron mass analyzer. We see no evidence for this in the clusters studied here, and instead attribute the decay to thermionic emission in the $I^-(NH_3)_n$, $I^-(CH_3OH)_n$, and $I^-(D_2O)_n$ clusters.

5. Conclusions

Femtosecond photoelectron spectroscopy has been used to examine the dynamics of small iodide–

solvent clusters excited to the cluster precursor to the charge-transfer-to-solvent state. We find significant variations in the electron solvation dynamics depending on the nature of the solvent. In $I^-(Xe)_n$ clusters, no significant solvent rearrangement occurs subsequent to CTTS excitation. The lower spin-orbit CTTS state is stable on the time-scale of the experiment (200 ps) while the upper CTTS state decays by spin-orbit-induced autodetachment. In contrast, the other solvents studied here do show evidence for partial solvation of the electron. $I^-(D_2O)_n$ clusters show the strongest dynamical variation with cluster size; five solvent molecules are required for solvation of the excess electron. The size-dependence of the electron solvation dynamics is more gradual for $I^-(NH_3)_n$ and $I^-(CH_3OH)_n$ clusters. In addition, excitation of $I^-(D_2O)_n$ clusters appears to initially populate a dipole-bound state, whereas no such state is evident in the FPE spectra of $I^-(NH_3)_n$ and $I^-(CH_3OH)_n$ clusters. By continuing to study CTTS bands in these and other clusters, we hope to make connection with the well-studied yet far from completely understood realm of solution-phase electron solvation.

Acknowledgements

This research is supported by the National Science Foundation under grant no. CHE-9732758. A.V.D. is a National Science Foundation predoctoral fellow. C.F. acknowledges post-doctoral support from the Deutsche Akademie der Naturforscher Leopoldina (grant BMBF-LPD 9801-6).

References

- [1] J. Franck, G. Scheibe, *Z. Phys. Chem. A* 139 (1928) 22.
- [2] E. Rabinowitch, *Rev. Mod. Phys.* 14 (1942) 112.
- [3] J. Jortner, M. Ottolenghi, G. Stein, *J. Phys. Chem.* 68 (1964) 247.
- [4] M.J. Blandamer, M.F. Fox, *Chem. Rev.* 70 (1970) 59.
- [5] F.H. Long, X. Shi, H. Lu, K.B. Eisenthal, *J. Phys. Chem.* 98 (1994) 7252.
- [6] Y. Gaudeul, H. Gelabert, M. Ashokkumar, *Chem. Phys.* 197 (1995) 167.
- [7] J.A. Kloepper, V.H. Vilchiz, V.A. Lenchenkov, S.E. Bradforth, *Chem. Phys. Lett.* 298 (1998) 120.

- [8] W.-S. Sheu, P.J. Rossky, *Chem. Phys. Lett.* 202 (1993) 186.
- [9] A. Staib, D. Borgis, *J. Chem. Phys.* 104 (1996) 9027.
- [10] D. Serxner, C.E. Dessent, M.A. Johnson, *J. Chem. Phys.* 105 (1996) 7231.
- [11] I. Becker, O. Cheshnovsky, *J. Chem. Phys.* 110 (1999) 6288.
- [12] I. Becker, G. Markovich, O. Cheshnovsky, *Phys. Rev. Lett.* 79 (1997) 3391.
- [13] B.J. Greenblatt, M.T. Zanni, D.M. Neumark, *Disc. Faraday Soc.* 108 (1997) 101.
- [14] L. Lehr, M.T. Zanni, C. Frischkorn, R. Weinkauff, D.M. Neumark, *Science* 284 (1999) 635.
- [15] T. Lenzer, M.R. Furlanetto, N.L. Pivonka, D.M. Neumark, *J. Chem. Phys.* 110 (1999) 6714.
- [16] C.G. Bailey, M.A. Johnson, *Chem. Phys. Lett.* 265 (1997) 185.